不锈钢点焊接头 S－N 曲线转折点的优化过渡

朱国仁[1]， 陈 松[2]， 王振宝[2]
(1. 吉林大学 链传动研究所，长春 130025; 2. 吉林大学 机械科学与工程学院，长春 130025)

摘 要：基于成组法、升降法试验，绘制出不锈钢点焊接头 S－N 曲线，根据所绘制的 S－N 曲线和升降法试验数据分析比较确定 S－N 曲线在转折点处需要进行转折过渡. 为了使制定出的 S－N 曲线和转折点疲劳寿命 N_0 具有更好的实际工程应用价值，提出了过渡点处采用变斜率斜线段连接的理论及方法. 通过试验验证了 S－N 曲线转折点处采用变斜率斜线段过渡方法的可行性，并对两条曲线进行了比较分析. 结果表明，利用新方法绘制的 S－N 曲线能更准确的显示点焊接头的性能.

关键词：点焊接头； S－N 曲线； 转折点； 变斜率斜线段过渡
中图分类号：TH 142.71; TG 453$^+$.9 **文献标识码**：A **文章编号**：0253－360X(2014)08－0035－04

0 序 言

点焊是融合了电、热、结构及相变的复杂过程，零件在电极力作用下形成零件与电极、零件与零件接触面，电流流经接触面产生焦耳热，使零件与零件的接触面熔化形成焊点[1]. 电阻点焊作为一门机械、力学、电子、控制等多学科密集交叉的专门制造技术，其发展与其它科技的进步息息相关[2]. 电阻点焊工艺在车体制造过程中得到了广泛应用，电阻点焊的疲劳特性有着至关重要作用. 点焊疲劳试验 S－N 曲线直观表达了点焊的疲劳特性，同时电阻点焊接头 S－N 曲线转折点疲劳寿命 N_0 是点焊接头重要的疲劳强度评价和设计的参数[3,4]. 在点焊接头 S－N 曲线转折点的处理中，国家标准 GB/T 3075—2008《金属材料—疲劳试验—轴向力控制方法》采和日本工业标准 JIS Z 3138—1989《点焊接头的疲劳试验方法》用简单的圆弧过渡，但在转折点过渡方式上没有给出相关参考内容和具体试验方法; 英国标准 BS 7608—1993《钢结构疲劳设计与评估》和国际标准 ISO 14324—2003《电阻点焊—焊接的损坏试验—点焊接头的疲劳试验方法》采用双对数坐标轴，没有对转折点 N_0 进行过渡处理. 文中选择了轨道列车不锈钢车体点焊接头试样，初步试验研究了点焊接头的 S－N 曲线转折点过渡形式和转折点过渡的试验方法及数据处理方法和理论，使制定出的 S－N 曲线和转折点疲劳寿命 N_0 具有更好的实际工程应用价值.

收稿日期：2013－07－01
基金项目：科技部国际合作资助项目(2009DFR80040)

1 S－N 曲线制定的理论和标准

线性损伤理论中 S－N 曲线由斜线段和疲劳极限水平直线段两部分组成[5]. 文中即以该理论作为基础进行研究.

国家标准 GB/T 3075—2008 和日本工业标准 JIS Z 3138—1989 规定点焊接头 S－N 曲线中转折点采用简单过渡，未涉及此处过渡形式和试验方法. 斜线段采用多载荷层不重复试样的拟合方法. 国际标准 ISO 14324—2003 和英国标准 BS 7608—1993 同样采用线性损伤理论，但在转折点不经过任何过渡处理，直接采用疲劳极限水平直线段与斜线段直接相交而得. 点焊接头疲劳试验 S－N 曲线制定只涉及了斜线段拟合和疲劳极限段拟合，并未涉及转折点的过渡. 疲劳试验中用疲劳极限段与斜线段相交得到转折点疲劳寿命 N_0，往往不能准确表达实际的转折点 N_0.

2 试样制备和试验设备确定

2.1 试样制备

文中采用轨道列车不锈钢车厢体电阻点焊接头试样进行疲劳试验，主要由车厢体中 3 个不同位置、不同厚度组合的 3 组试验试样. 根据国家标准GB/T 15111—94《点焊接头剪切拉伸疲劳试验方法》制定试板及试件，试件是由两块或三块等长的宽度为 45 mm 的不锈钢板电阻点焊而成. 3 组不锈钢车体上点焊接头组合如表 1 所示. 焊缝质量等级执行欧洲标准 EN 15085—3《铁路应用——轨道机车车辆以

及轨道机车车辆部件的焊接》中 CP C2 级，焊接公差标准执行国际标准 ISO 13920《焊接——焊接结构的一般公差——长度和角度的尺寸——形状和位置》中的 A 级，点焊痕迹深度不超过单侧板厚度的 10%.

表 1 试样规格

Table 1 Sample Specification

编号	板厚组合 L/mm	总厚度 h/mm	焊核直径 d/mm
1	1-SUS301L-HT + 3-SUS301L-ST + 2-SUS301L-HT	6	5
2	2-SUS301L-ST + 2-SUS301L-DLT	4	7
3	2-SUS301L-HT + 3-SUS301L-ST + 2-SUS301L-ST	7	7

2.2 试验设备

材料试验机型号为 WE—30 型液压万能试验机，载荷示值误差小于等于 ±1%；疲劳试验机型号为 PLG—20C 型高频拉压疲劳试验机，载荷示值误差小于等于 ±1%. 在室温空气介质中进行，等幅正弦曲线变化的剪切拉压，试验频率为 50 ~ 100 Hz，给定极限疲劳寿命 10^7 周次.

3 S – N 曲线和转折点的制定

3.1 点焊接头 S – N 曲线的制定

以 1 号试样为例，取疲劳试验循环特性系数为 0.1. 根据成组法和升降法得到 1 号试样的 S – N 曲线[6,7].

图 1 斜线段与疲劳极限段相交所得平均值 S – N 曲线转折点 N_0 疲劳寿命为 5.49×10^5 周次. 而实际转折点疲劳寿命可以根据升降法中疲劳寿命大致确定，1 号试样升降法数据如表 2 所示.

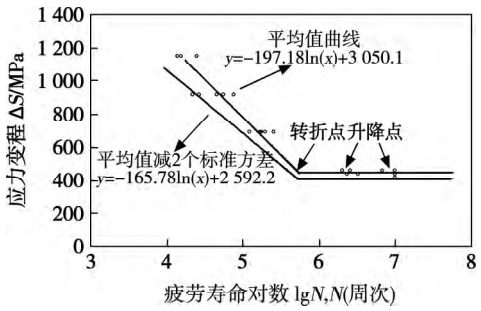

图 1 1 号试样 S – N 曲线

Fig. 1 Sample No. 1 S – N curve

从升降法数据或者图 1 中容易得到，1 号试样直接用斜线段与疲劳极限段相交得到转折点 N_0，大大低于升降法中疲劳寿命，不能很好地拟合和表达升降法中相关数据，即与实际 S – N 曲线的转折点不符，不能满足工程的实际需要. 转折点处需要进行优化过渡.

表 2 1 号试样升降法数据

Table 2 Sample No. 1 ladder method data

应力变程 ΔS/MPa	疲劳寿命 N(10^6 周次)			
481.330	0.772	0.960	—	—
459.447	2.580	10.000	6.77	2.02
437.571	10.000	10.000	3.25	2.32
415.696	10.000	10.000	—	—

3.2 点焊接头 S – N 曲线转折点疲劳寿命 N_0 分析

1 号试样转折点相交得到 N_0，不能准确表达试验数据，同理根据其余 2 组不同组合试样试验数据，与升降法得到实际疲劳寿命数据进行比较，得到相关转折点 N_0 数据如表 3 所示.

表 3 平均值 S – N 曲线转折点 N_0

Table 3 Average S – N curve turning point N_0 data

转折点疲劳寿命 N_0(10^5 周次)		升降法试验数据				
		应力变程 ΔS/MPa	疲劳寿命 N(10^6 周次)			
2 号试样	8.06	203.83	1.68	3.20	—	—
		194.56	2.24	1.63	2.05	10
		185.30	4.08	10.00	1.55	—
		176.03	10.00	10.00	—	—
3 号试样	3.66	280.76	4.00	—	—	—
		268.00	7.06	6.31	10.00	—
		255.23	9.52	1.94	10.00	—
		242.47	6.40	10.00	10.00	—

从表 3 中可以看出，试样转折点疲劳寿命都未达到 10^6 周次这一数量级. 而在大部分情况下，疲劳极限段的疲劳寿命应该大于 10^6. 表 3 中数据得知，所有不同组合试样，转折点疲劳寿命低于升降法中实际试样疲劳寿命，不能准确拟合试验数据和表达疲劳极限载荷下疲劳寿命.

4 试验结果

4.1 转折点过渡区域补充试样

1 号试样在转折点 N_0 附近进行探索试验. 在 529.73，575.75，621.78 MPa 3 个载荷层下进行补充试验. 其试验结果如表 4 所示.

表 4　过渡区域补充试样数据

Table 4　Complementary specimen data in transition area

应力变程	疲劳寿命		疲劳寿命平均值	平均值减 2 个标准方差
$\triangle S$/MPa	N(10^5 周次)		N_1(10^5 周次)	N_2(10^5 周次)
529.73	5.53	3.61	4.57	2.65
575.75	4.06	3.18	3.62	2.37
621.78	2.55	1.86	2.20	1.23

得到如下加入补充试样数据点的 S－N 曲线，如图 2 所示.

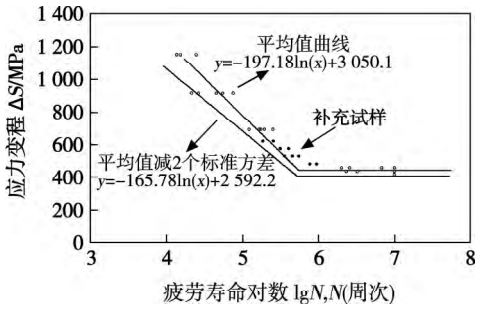

图 2　1 号试样加入补充试样 S－N 曲线

Fig. 2　Additional sample No. 1 S－N curve

4.2　直线过渡方式的提出

文中初步提出引进直线过渡方式. 直线相对其它线性曲线的简易性，使得直线过渡比其它线性过渡方式具有更好的直观性和表达性. 通过对线性回归方程进行显著性检验和确定系数 R^2，验证直线过渡方式的可行性. 对补充 4 个应力载荷下疲劳寿命的平均值和平均值减 2 个标准方差引进一元线性回归模型进行初步的过渡研究.

一元线性回归模型为

$$y=\beta_0+\beta_1\ln(x)+e \tag{1}$$

式中：y 为应力变程 ΔS；x 为疲劳寿命 N；e 为不能用 $\beta_0+\beta_1\ln(x)$ 所表示的部分. 应用最小二乘法计算得到补充试样两条经验回归曲线如图 3 所示. 平均值 $\bar{x}$ 回归曲线 $y=-100.09\ln(x)+1\,846.7$，平均值减 2 个标准方差 $\bar{x}-2s$ 回归曲线 $y=-89.853\ln(x)+1\,672.9$

通过对补充试样区域进行过渡处理，得到两条曲线与水平疲劳极限段相交转折点：疲劳寿命平均值拟合曲线转折点(1.22×10^6 周次，444.13 MPa)；疲劳寿命平均值减 2 个标准方差拟合曲线转折点(1.31×10^6 周次，407.53 MPa)；从图 3 中拟合情况可知，通过直线过渡后点焊接头 S－N 曲线的转折点更为符合实际数据，曲线拟合程度更高，更具参考价值.

4.3　直线过渡方式的可行性验证

补充试样平均值回归方程的显著性检验. 方差

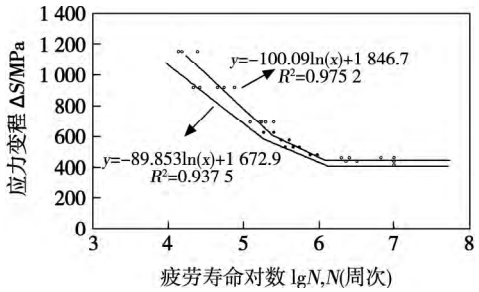

图 3　1 号试样过渡区域补充后 S－N 曲线

Fig. 3　Sample No. 1 S－N curve of transition area add specimen

分析如表 5 所示.

表 5　补充试样平均值方差分析

Table 5　Analysis table of additional sample average variance

方差源	平方和 S	自由度 U	均方 M	F 值 F
回归	10 610.28	1	10 610.28	—
误差	313.18	2	156.59	67.76
总和	10 923.46	3	—	—

对给定的水平 $\alpha=0.05$，查 F 分布临界表得 $F_{1,2}=18.51$，因 $F=67.76>18.51$，应该接受 $\beta_1\neq0$. 认为经验回归曲线 $y=-197.18\ln(x)+3\,050.1$ 反应了疲劳寿命平均值下应力变程 ΔS 与疲劳寿命 N 之间的相关关系.

同理得到补充试样平均值减 2 个标准方差回归方程的 F 值：$F=29.93>18.51$. 同样认为经验回归曲线 $y=-89.853\ln(x)+1\,672.9$，反映了疲劳寿命平均值减去 2 个标准方差下应力变程 ΔS 与疲劳寿命 N 之间的相关关系.

另一方面，计算出补充试样疲劳寿命平均值回归方程 $R^2=0.975\,2$；补充试样疲劳寿命平均值减 2 个标准方差回归方程 $R^2=0.937\,4$. 这表明在直线拟合曲线下，两条拟合曲线有 97.52%，93.74% 的变化是由应力变程 ΔS 与疲劳寿命 N 的线性关系引起的[8].

5　讨　　论

采用文中 1 号试样过渡区域密集试样试验的方法得到过渡直线段，在实际试验过程中大大增加了试样数量和试验时间. 拟采用国际标准 ISO 14324—2003 中多载荷层，不重复试样的方法，对转折点过渡区域进行试验，能减少试样数量和试验

时间.

在转折点处采用过渡方式,主要是想得到一个较为可靠的转折点处疲劳寿命 N_0,因此以图2中得到的转折点 N_0 作为实际参考值,应用多载荷层,不重复试样的方法,对1号试样过渡区域的试样数据进行分析比较,以确定试验方法的可行性. 采用与转折点较为接近的3个载荷层 481.33,529.73,575.75 MPa 水平下不重复试样进行单个试样试验. 根据1号试样转折点过渡区域的试验数据,3个载荷层下选择单点组合,可以得到不重复试样下的两个转折点极值疲劳寿命 N_0.

通过试样点(9.60×10^5 周次,481.33 MPa),(5.53×10^5 周次,529.73 MPa),(3.18×10^5 周次,575.75 MPa),经过最小二乘法拟合得到过渡极限曲线 $y=-85.458\ln(x)+1\ 658.9$,得到极限转折点 $N_{01}=1.324\times10^6$;通过试样点(7.72×10^5 周次,481.33 MPa),(4.57×10^5 周次,529.73 MPa),(4.06×10^5 周次,575.75 MPa),经过最小二乘法拟合得到过渡极限曲线 $y=-130.37\ln(x)+2\ 245.7$. 得到极限转折点 $N_{02}=1.003\times10^6$ 周次.

极限转折点 N_{01},N_{02} 与曲线得到的平均值过渡转折点 $N'_{01}=5.37\times10^5$ 周次和平均值经直线过渡转折点 $N'_{02}=1.22\times10^6$ 周次比较,得知 N_{01},N_{02} 在一个较为合理的范围,与实际经直线过渡转折点 N_0 绝对误差控制在20%范围内. 可知通过3个载荷层,3个试样,不重复试样试验的方法,就能较好的表达出实际需求的转折点过渡.

6 结 论

(1) 疲劳试验中,实际试验数据所得到的转折点疲劳寿命高于未经过渡处理的 S-N 曲线中疲劳极限直线段和斜线段直接相交所得转折点 N_0 的疲劳寿命.

(2) 点焊接头试样疲劳试验 S-N 曲线转折点 N_0 处可采用直线拟合进行过渡. 采用两条斜线段双斜率曲线拟合,能准确表达出实际转折点 N_0,具有更高的工程实用价值.

(3) 转折点直线过渡方式采用多载荷层,不重复试样的试验方法,能较好的表达出实际需求的转折点过渡,减少了试验时间和试样数量,满足实际试验要求.

参考文献:

[1] 林忠钦,胡 敏,米新民,等. 轿车白车身点焊装配过程有限元分析[J]. 焊接学报,2001,22(1):36-40.
Lin Zhongqin, Hu Min, Mi Xinmin, *et al*. FEM analysis or spot welding process in autobody manufacturing [J]. Transactions of the China Welding Institution, 2001, 22(1): 36-40.

[2] 曹海鹏,赵熹华,赵 贺. 铝合金电阻点焊工艺设计自动化[J]. 焊接学报,2005,26(2):21-24.
Cao Haipeng, Zhao Xihua, Zhao He. Intelligent process design of resistance spot welding of aluminum alloys [J]. Transactions of the China Welding Institution, 2005, 26(2): 21-24.

[3] 赵少汴. S-N 曲线转折点疲劳寿命 N_0 的探讨[J]. 机械强度,2001,23(1):22-24.
Zhao Shaobian. Study on the cycles N_0 corresponding to the breaking point of the S-N curve [J]. Journal of Mechanical Strength, 2001, 23(1): 22-24.

[4] 范文学,陈芙蓉,解瑞军,等. 基于不同 S-N 曲线的横向十字焊接接头疲劳寿命预测[J]. 焊接学报,2013,34(11):69-72.
Fan Wenxue, Chen Furong, Xie Ruijun, *et al*. Fatigue life prediction of transverse cross welded joint based on different S-N curve [J]. Transactions of the China Welding Institution, 2013, 34(11): 69-72.

[5] Collins J A. Failure of materials in mechanical design [M]. New York: Wiley-Interscience, 1993.

[6] 高镇同. 疲劳应用统计学[M]. 北京:国防工业出版社,1986.

[7] Maddox S J. Review of fatigue assessment procedures for welded aluminum structures [J]. International Journal of Fatigue, 2003, 25: 1359-1378.

[8] 王松桂. 概率论与数理统计[M]. 北京:科学出版社,2011.

作者简介:朱国仁,男,1965年出生,学士,高级工程师. 主要从事先进测试方法和数据处理先进测试设备等方面研究. 发表论文25篇. Email: zhugr@jlu.edu.cn

Hot corrosion resistance of plasma-sprayed MCrAlY coatings by laser remelting on TiAl alloy surface WANG Dongsheng[1,2], TIAN Zongjun[1], SHEN Lida[1], HUANG Yinhui[1] (1. College of Mechanical and Electrical Engineering, Nanjing University of Aeronautics and Astronautics, Nanjing 210016, China; 2. College of Mechanical Engineering, Tongling University, Tongling 244000, China). pp 17 - 20

Abstract: The MCrAlY coatings were prepared by plasma spraying on TiAl alloy surface, laser remelting experiment had been carried out and the hot corrosion resistance of TiAl alloy, plasma-sprayed and laser-remelted MCrAlY coatings in 5% Na_2SO_4 + 25% NaCl (mass fraction) molten salt at 850 ℃ were researched. The hot corrosion failure mechanisms of three kinds of materials were analyzed and the influence of laser remelting on hot corrosion behavior of plasma-sprayed MCrAlY coating were discussed. The results show that the plasma-spayed MCrAlY coating has better oxidation resistance than the original TiAl alloy, and the laser-remelted coating has the best oxidation resistance. The hot corrosion of MCrAlY coating included surface oxidation and internal sulfide, and produced Al_2O_3, Cr_2O_3, NiO, $NiCr_2O_4$, Ni_3S_2 and CrS et al.

Key words: laser remelting; plasma spraying; MCrAlY coating; TiAl alloy; hot corrosion resistance

Experiment on metal transfer control of laser enhanced GMAW welding ZHU Jialei, JIAO Xiangdong, QIAO Xi, JIA Cunfeng (Mechanical Engineering College, Beijing Institute of Petrochemical Technology, Beijing 102600, China). pp 21 - 24, 29

Abstract: Underwater ambient pressure has negative effect on metal transfer and welding processing stability, so extra force is needed to help to stabilize welding arc and improve metal transfer state during underwater welding. To verify the feasibility of laser which enhanced metal transfer control, the related experiment system was built at atmospheric pressure, and contrastive study on metal transfer state with and without laser enhanced was conducted. Results showed that the application of a certain power density of laser could improve metal transfer behavior obviously and the size of droplet could be controlled by laser, the welding stability also could be improved. The result laid a foundation for the further laser enhanced hyperbaric underwater welding experiment.

Key words: laser enhanced; metal transfer; high-speed photograph; experiment

Study on the softening of 6005A-T6 aluminum alloy welding joints for high-speed train LÜ Xiaochun[1], LEI Zhen[1], ZHANG Jian[1], ZHANG Lihua[2] (1. Harbin Welding Institute, China Academy of Machinery Science & Technology, Harbin 150028, China; 2. XCMG Construction Machinery Co., Ltd. Building Machinery Co., Xuzhou 221004, China). pp 25 - 29

Abstract: Welding thermal cycle curves of 6005A-T6 aluminum alloy by using tandem MIG welding and laser-tandem MIG hybrid welding was tested individually. The softening of the welding joints was studied through welding thermal simulation with heat treatment method. The test results demonstrated that the notable softening in HAZ began as long as the peak temperature of welding thermal cycle curve exceeded 260 ℃, and the most serious softening in HAZ occurred while the peak temperature of welding thermal cycle curve was up to 350 ℃. The unstable phase of β'' and β', the main strengthening phase of 6005A-T6 aluminum alloy, transformed to β (Mg_2Si) which aggregated and grew to block was the main reason why the softening happened. The hardness of the joints in HAZ, where the peak temperature of welding thermal cycle curve was between 260 - 500 ℃, could not recover totally through ageing treatment. The detention time beyond 260 ℃ on the thermal cycle curve of laser-tandem MIG hybrid welding joints was much shorter than that of tandem MIG welding joints, so that the softening of laser-tandem MIG hybrid welding joints was little slighter than that of tandem MIG welding joints.

Key words: high-speed train; 6005A aluminum alloy; laser hybrid welding; softening of welding joints

An improved three-dimensional reconstruction algorithm for microelectronics assembly solder joint ZHAO Huihuang[1,2], WANG Yaonan[1]. SUN Yaqi[2], WEI Shudi[2] (1. College of Electrical and Information Engineering, Hunan University, Hunan 410082, China; 2. Department of Computer Science, Hengyang Normal University, Hengyang 421008, China). pp 30 - 34, 42

Abstract: Solder joint three-dimensional (3D) reconstruction is one of the key research of microelectronic assembly quality 3D detection and control technology development. During the solder joint 3D reconstruction based on SFS theory, its 3D reconstruction becomes one of the key problems because of existing "high light area" on solder joint surface. In order to resolve the problem, at first, by analyzing the reflection items on solder joint surface, a reflection model is got for microelectronics solder joint according to the characteristics of joint surface and solder joint image. Then, by analyzing the formation principle of "high light area" and modifying the reconstruction result, an improved 3D reconstruction algorithm is proposed for microelectronics assembly solder joint. At last, the experimental results have shown that the "distortion" can be solved and the 3D shape based on the improved illumination model is more satisfactory in decreasing specular reflection influence than that of the traditional methods.

Key words: solder joint; microelectronics assembly; three-dimensional reconstruction; shape from shading

Optimization of transition in stainless steel welding joints S-N curve breaking point ZHU Guoren[1], CHEN Song[2], WANG Zhenbao[2] (1. Chain Transmission Institute, Jilin University, Changchun 130025, China; 2. Institute of Mechanical Science and Engineering, Jilin University, Changchun 130025, China). pp 35 - 38

Abstract: Based on the ladder method and the group method, the S - N curve of stainless steel welding fittings was drawn. According to comparing drawn S - N curve with the ladder

method data, the turning point of S－N curve requires turning transition. In order to make the S－N curve and the breaking point N_0 have more engineering application value, the theory and method of transition point connected with variable slope curve was proposed. The feasibility of using variable slope method has been verified by experiment, and the two curves were compared by analysis . The results show that the new method of drawing the S－N curve can display the performance of welding joints spot more accurately.

Key words: spot welded joints; S－N curve; breaking point N_0; variable slope slash transition

Analysis of vibration fatigue S－N curve on Q235B steel butt welded joint FAN Wenxue[1,2], CHEN Furong[1], XIE Ruijun[1], TANG Dafu[1] (1. Institute of Materials Science and Engineering, Inner Mongolia University of Technology, Hohhot 010051, China; 2. Mining Institute, Inner Mongolia University of Technology, Hohhot 010051, China). pp 39－42

Abstract: The interrelation of static fatigue S－N curve and vibration fatigue S－N curve on Q235B steel butt welded joints has been analyzed. The result shows they have the same slope, and vibration fatigue S－N curve is a continuous curve without horizontal section. It moves a specified distance in stress axis. At the same time, the vibration fatigue S－N curve expression was input. In this paper, the static fatigue test and tensile test under different load frequency were done. And vibration fatigue correction factor was 0.345 2. Through correction of residual stress and size, the fatigue limit was 114.84 MPa when the cycles were 5×10^6 under vibration fatigue S－N curve. And it only has a little bias 7.60%, it shows that the method of this paper can be used to infer vibration fatigue S－N curve of Q235B steel.

Key words: Q235B steel welded joint; vibration fatigue; S－N curve

Formation process of hot cracking in copper He shielding gas tungsten welding LI Yinan[1], YAN Jiuchun[2], GUO Feng[1], PENG Zilong[1] (1. Department of Mechanical Engineering, Qingdao Technological University, Qingdao 266033, China; 2. State Key Laboratory of Advanced Welding Production Technology, Harbin Institute of Technology, Harbin 150001, China). pp 43－47

Abstract: The formation mechanism of hot cracking in gas tungsten arc welding (GTAW) of copper structures in large dimensions was researched. The dynamic formation process of hot cracking was observed and analyzed. The formation criterion of hot cracking was optimized based on the Prokhorov's theory, and the finite element model of thick copper plates in GTA welding was established based on the rigid restraint cracking test. It is concluded that the internal deformation rate $\Delta\varepsilon$ is the internal reason of forming hot cracking. The variation of the transverse tensile stress and the $\Delta\varepsilon$ in brittle temperature range (BTR) was obtained. And the formation mechanism of hot cracking without preheating was carried out compared $\Delta\varepsilon$ with high temperature ductility of HS201 welded metal. The variation of $\Delta\varepsilon$ in difference preheating temperature was analyzed to prevent hot cracking forming, and it can be concluded that the $\Delta\varepsilon$ in BTR could be declined by preheating process and the cracking susceptibility will be decreased.

Key words: copper; hot cracking; gas tungsten arc welding

Modeling and control of the nonlinear joints system of mobile repair welding robot LIU Jiajun[1], SUN Zhenguo[1], ZHANG Wenzeng[1], CHEN Qiang[1,2] (1. Key Laboratory for Advanced Materials Processing Technology, Department of Mechanical Engineering, Tsinghua University, Ministry of Education, Beijing 100084, China; 2. Yangtze Delta Region Institute of Tsinghua University, Jiaxing 314006, China). pp 48－52

Abstract: Highly nonlinear units such as deadzone and backlash exist in the joints of mobile repair welding robot, which have negative effects on control accuracy. To improve the path control accuracy of the end effector, Particle swarm optimization algorithm is used to identify the model of the nonlinear joints system. Then switching compensation control method referring the identified model is applied to the joint controlling system, combined with feedfoward-feedback control based on inverse kinematics, the hybrid control method realize considerable path accuracy. Experiments show that the average path error of designed welding robot's end effector is less than 0.2 mm with this control method, and the shortcomings of low precision reducer are compensated.

Key words: mobile welding robot; nonlinear system; identification; backlash compensation; feedforward

Feature characters extraction with visual attention method based on three-light-path weld pool images ZHANG Yan, LÜ Na, HUANG Yiming, CHEN Shanben (Intelligentized Robotic Welding Technology Laboratory, Shanghai Jiaotong University, Shanghai 200240, China). pp 53－56

Abstract: Seam tracking and weld penetration control are key parts of weld quality control. A three-light-path vision sensing system is used in the experiments to obtain the images of the top-front, top-back and back paths of the weld pool during the Al alloy GTAW welding and project them in the same picture at the same time. The image contains information of the seam, weld pool and back weld pool. The method of visual attention is adopted to find the small areas related to weld pool feature characters, and extract these characters from the image. The results show that, in real-time detection of the weld pool features during the welding process, the method of visual attention is more clarified and efficient than general methods as it focuses only on interested small areas.

Key words: welding quality control; weld pool image processing; visual attention; region of interest detection

Investigation on three-dimensional real coupling numerical simulation of temperature field of friction stir welding of 2219 aluminum alloy DU Yanfeng[1,2], BAI Jingbin[1], TIAN Zhijie[1], LI Jinsong[1], ZHANG Yanhua[2] (1. Capital Aerospace